Front. Chem. Sci. Eng. 2022, 16(2): 303–315
https://doi.org/10.1007/s11705-021-2044-z

RESEARCH ARTICLE

Energy-efficient recovery of tetrahydrofuran and ethyl acetate by triple-column extractive distillation: entrainer design and process optimization

Ao Yang[1,2], Yang Su[3], Tao Shi[2], Jingzheng Ren[2], Weifeng Shen (✉)[1], Teng Zhou (✉)[4,5]

1 School of Chemistry and Chemical Engineering, Chongqing University, Chongqing 401331, China
2 Department of Industrial and Systems Engineering, The Hong Kong Polytechnic University, Hong Kong, China
3 School of Intelligent Technology and Engineering, Chongqing University of Science & Technology, Chongqing 401331, China
4 Process Systems Engineering, Otto-von-Guericke University Magdeburg, D-39106 Magdeburg, Germany
5 Process Systems Engineering, Max Planck Institute for Dynamics of Complex Technical Systems, D-39106 Magdeburg, Germany

Abstract An energy-efficient triple-column extractive distillation process is developed for recovering tetrahydrofuran and ethyl acetate from industrial effluent. The process development follows a rigorous hierarchical design procedure that involves entrainer design, thermodynamic analysis, process design and optimization, and heat integration. The computer-aided molecular design method is firstly used to find promising entrainer candidates and the best one is determined via rigorous thermodynamic analysis. Subsequently, the direct and indirect triple-column extractive distillation processes are proposed in the conceptual design step. These two extractive distillation processes are then optimized by employing an improved genetic algorithm. Finally, heat integration is performed to further reduce the process energy consumption. The results indicate that the indirect extractive distillation process with heat integration shows the highest performance in terms of the process economics.

Keywords extractive distillation, solvent selection, conceptual design, process optimization, heat integration

1 Introduction

Tetrahydrofuran (THF) and ethyl acetate (EtAC) are regularly used as organic solvents and biofuels as well as sustainable biomass energy sources for the internal combustion engines [1,2]. According to the report from He et al. [3], wastewater mixtures containing THF and EtAC are generally produced in the chemical and pharmaceutical industries. However, the separation of such mixtures is difficult via the conventional distillation process because the distillation boundary and multiple azeotropes exist in this system. Thereby, the explorations of efficient processes for separating such mixtures are significant in realizing the recovery of available resources and reducing the environmental pollution [4,5].

Extractive distillation (ED) [6,7], pressure-swing distillation [8,9] and azeotropic distillation [10,11] are employed as effective approaches to separate azeotropic mixtures. Pressure-swing distillation is limited to pressure-sensitive systems [12] and multiple steady-states can exist in the azeotropic distillation process [13]. Therefore, the ED process becomes one of the most popular separation techniques for handling azeotropic or close-boiling systems in the chemical and petroleum industries due to its advantage in the operational and control aspects [14,15]. For example, Yang et al. [16] reported an ED process to separate the binary azeotropic mixture dimethyl carbonate and ethanol by varying the operating pressures. Shi et al. [17] explored the separation of the ternary mixture isopropyl alcohol/isopropyl acetate/water with multiple azeotropes via two-alternative ED schemes. The separation of azeotropic systems has also been investigated by other researchers [18–20] using ED.

The selection of entrainer plays a key role in designing the energy-saving ED processes [21,22]. Cui et al. [23] studied the separation performance of two different entrainers via phase diagram analysis and they found that ethylene glycol is more suitable for the separation of benzene/isopropanol/water by ED. Zhu et al. [24] developed a heuristic method employing the relative volatility to determine the optimal solvent with the best economic

Received November 8, 2020; accepted January 27, 2021

E-mails: shenweifeng@cqu.edu.cn (Shen W),
zhout@mpi-magdeburg.mpg.de (Zhou T)

performance. Shen et al. [25] proposed a solvent selection approach employing five properties (i.e., relative volatility, solubility power, molecular weight, melting point and boiling point) as objectives to screen the best entrainer. Blahušiak et al. [26] developed another quick calculation procedure for the preselection of solvents by considering the minimum energy consumption and solvent-to-feed ratio. The efficiency and reliability of this method were successfully verified via several industrial application cases. Unfortunately, these previous works all considered a limited, pre-specified solvents and tried to find the best candidate from these solvents. In comparison with the previous solvent screening methods, the computer-aided molecular design (CAMD) method developed by Gani and Brignole [27] attempts to rationally design the most suitable solvents [28–33] from a list of molecular building groups. Recently, Zhou et al. [34] proposed a multi-objective CAMD approach to design solvents for the separation of binary azeotropic mixture *n*-hexane/methanol. In the present work, we use this method to find potential entrainers for the ternary azeotropic system THF/EtAC/water. Subsequently, thermodynamic insights are employed to further determine the best entrainer for the ED process.

In addition to the optimal selection of solvent, energy saving could be further achieved by the process optimization technique [35]. Waltermann et al. [36] formulated extractive and heteroazeotropic distillation process design tasks into mixed-integer nonlinear programming (MINLP) problems and solved them as a series of successively relaxed nonlinear programming problems. Krone et al. [37] proposed a superstructure-based modeling environment to facilitate the MINLP optimization of complex distillation processes where rigorous thermodynamic models are used. It should be noted that conventional gradient-based optimization algorithms are not efficient for handling complex MINLP problems in distillation processes with massive coupled discrete and continuous decision variables [38]. By contrast, stochastic or hybrid optimization algorithms can be very powerful for solving these problems [39]. For example, Kruber et al. [40] optimized ED processes using a hybrid evolutionary-deterministic optimization approach. Yang et al. [41] optimized a thermally coupled ED process via the genetic algorithm (GA). You et al. [42] discussed the optimization of the ED process by using the sequential quadratic programming and GA approaches and they proved that the process economic performance can be further improved via the GA-based optimization.

In this work, we develop an efficient ED process to recover THF and EtAC from industrial wastewater. A rigorous hierarchical design procedure involving entrainer design, thermodynamic analysis, process design and optimization, and heat integration is followed in the process development. Specifically, candidate entrainers for the separation of THF/EtAC/water are first screened via the CAMD method. The iso- and uni-volatility lines between the azeotropic mixture and the entrainer are compared to obtain the most efficient entrainer for the separation task. Subsequently, volatility orders and distillation sequences (i.e., direct and indirect separation flowsheets) are determined in the conceptual design step. An improved GA is then employed to optimize the direct and indirect ED processes. Finally, heat integration is performed to further reduce the energy consumption of the processes.

2 Methodology

A systematic approach (as illustrated in Fig. 1) involving the selection of entrainer via CAMD and thermodynamic analysis, conceptual design, process optimization, and heat integration is proposed to find an energy-efficient ED process for the separation of the ternary azeotropic mixture THF/EtAC/water. In Step 1, candidate entrainers are first designed via the CAMD method and then the most suitable entrainer is determined via the comparison of iso- and uni-volatility lines of the ternary phase diagrams. In Step 2, the conceptual design of the ED process considering the direct and indirect separation sequences is performed via the rigorous thermodynamic analysis. In Step 3, an improved GA is used to optimize the operating variables (e.g., total number of stages and reflux ratios) for both direct and indirect separation processes. Finally, in Step 4, heat integration is performed for the optimized processes to further reduce the energy consumptions.

2.1 Screening of entrainer

2.1.1 Computer-aided entrainer design

The entrainer plays a significant role in the ED process [43]. In this work, the CAMD approach is employed to obtain the potential candidate entrainers. In total, twenty-two UNIFAC-Dortmund (UNIFAC-DMD) groups for building the entrainer molecules are considered in this work. Their UNIFAC-DMD group IDs, valences, and maximum occurrences are listed in Table 1. The van der Waals volume R_j and surface area Q_j are summarized in Table S1 (cf. Electronic Supplementary Material, ESM).

Following the study of Zhou et al. [34], the solvent infinite dilution selectivity (S_{AB}^{∞}) and infinite dilution capacity toward B (C_B^{∞}) as shown in Eqs. (1) and (2) can be used in the CAMD program to find promising entrainers for the separation of B from A using ED. Herein, due to the trade-off between these two selection criteria, we introduced a weighted function, displayed in Eq. (3), as our final objective function.

$$S_{AB}^{\infty} = \frac{\gamma_A^{\infty}}{\gamma_B^{\infty}}, \tag{1}$$

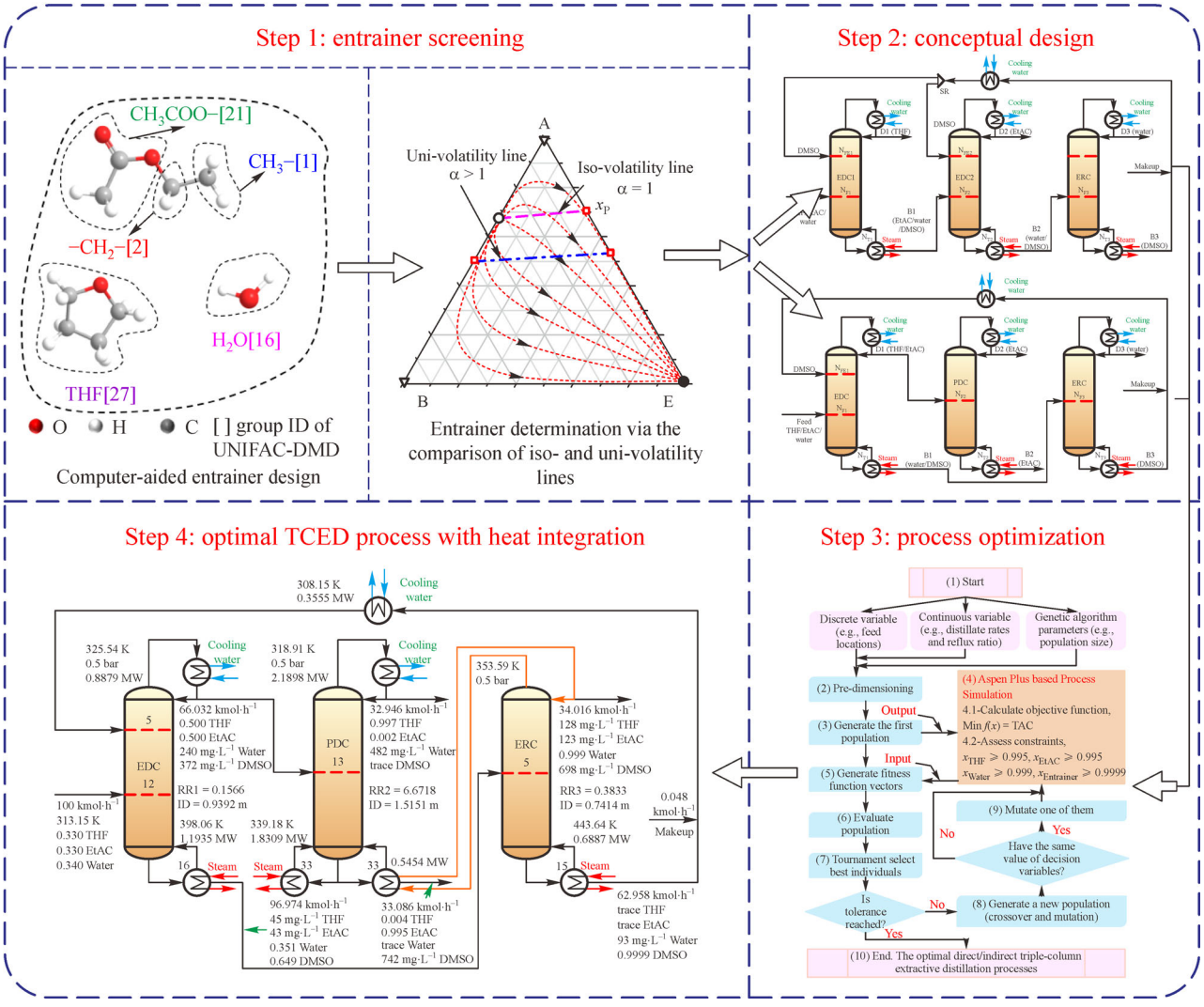

Fig. 1 Systematic approach for conceptual design and optimization of the THF/EtAC/water separation process.

$$C_{\mathrm{B}}^{\infty}=\frac{1}{\gamma_{\mathrm{B}}^{\infty}}, \tag{2}$$

$$\text{Objective function}=\max\left(\omega_1 S_{\mathrm{AB}}^{\infty}+(1-\omega_1)C_{\mathrm{B}}^{\infty}\right), \tag{3}$$

where ω_1 and $(1-\omega_1)$ represent the weight coefficients of S_{AB}^{∞} and C_{B}^{∞}, respectively. In the CAMD approach, ω_1 is a variable from 0.0 to 1.0 with a step size of 0.1. $\gamma_{\mathrm{A}}^{\infty}$ and $\gamma_{\mathrm{B}}^{\infty}$ are the infinite dilution activity coefficients of A and B in the entrainer, respectively. They can be calculated using the UNIFAC-DMD model at the infinite dilution condition. In this work, the ternary mixture being separated has two azeotropes, THF/water and EtAC/water. Thereby, A and B indicate the THF (or EtAC) and water, respectively.

The molecular structure should be constrained in the CAMD to ensure that the generated molecule is structurally feasible and uncomplicated. The structural feasibility and complexity rules are taken directly from Zhou et al. [34]. The upper limit of the total number of groups in the solvent molecule is set to 6. Melting and boiling points are used as the property constraints. The melting point as shown in Eq. (4) is used to ensure that the designed molecules are liquid at room temperature. In the ED process, the entrainer is recovered via distillation. Thereby, lower and upper bounds (Eq. (5)) are employed to constrain the normal boiling point of the entrainer.

$$\sum_{j=1}^{N} n_j t_{\mathrm{m},j} \leqslant \exp\left(\frac{T_{\mathrm{m}}^{\mathrm{upper}}}{T_{\mathrm{m0}}}\right), \tag{4}$$

$$\exp\left(\frac{T_{\mathrm{b}}^{\mathrm{lower}}}{T_{\mathrm{b0}}}\right) \leqslant \sum_{j=1}^{N} n_j t_{\mathrm{b},j} \leqslant \exp\left(\frac{T_{\mathrm{b}}^{\mathrm{upper}}}{T_{\mathrm{b0}}}\right), \tag{5}$$

where n_j is the number of group j present in the entrainer molecule and N denotes the total number of groups considered in this work (N = 22, see Table 1). The upper

Table 1 Functional groups and single-group molecules with their IDs, valences, and maximum numbers

Group ID	Group *j*	Valence *v*(*j*)	Group classification
1	CH_3	1	Mg [a]
2	CH_2	2	Mg [a]
3	CH	3	Mg [a]
4	C	4	Mg [a]
14	OH(P)	1	Ceg [b]
15	CH_3OH	0	Sg [c]
16	H_2O	0	Sg [c]
18	CH_3CO	1	Ceg [b]
19	CH_2CO	2	Nceg [d]
20	CHO	1	Ceg [b]
21	CH_3COO	1	Ceg [b]
22	CH_2COO	2	Nceg [d]
23	HCOO	1	Ceg [b]
24	CH_3–O	1	Ceg [b]
25	CH_2–O	2	Nceg [d]
26	CH–O	3	Nceg [d]
27	THF	0	Sg [c]
61	Furfural	0	Sg [c]
67	DMSO	0	Sg [c]
72	DMF	0	Sg [c]
81	OH(S)	1	Ceg [b]
82	OH(T)	1	Ceg [b]

a) Mg: main groups; b) Ceg: chain-ending function groups; c) Sg: single-group molecules; d) Nceg: non chain-ending function groups.

temperature of the melting point (T_m^{upper}) is 315 K; the lower and upper bounds of the boiling point (T_b^{lower} and T_b^{upper}) are 393.15 K and 493.15 K; T_{m0} and T_{b0} are 147.45 K and 222.54 K, respectively. Group contributions $t_{m,j}$ and $t_{b,j}$ can be found from Marrero and Gani [44]. The detailed formulation of the CAMD problem can be found in Zhou et al. [34]. The resulting mixed-integer optimization problem is coded and solved in Python.

2.1.2 Solvent determination via the thermodynamic analysis

The suitable entrainer of the ED process could be further determined via the thermodynamic feasibility analysis. Figure 2 illustrates the residue curve maps (RCMs) of the EtAC/THF/water, EtAC/water/E and THF/water/E systems where E indicates an arbitrary effective entrainer. As shown in Fig. 2(a), there are two azeotropes (one between THF and water and the other between EtAC and water). Their azeotropic temperatures are 335.74 K and 344.61 K and the corresponding azeotropic compositions are 78.72 and 61.32 mol-%, respectively. The black dot, hollow triangle and hollow circle represent the stable node, saddle and unstable node, respectively. In Fig. 2(a), the ternary diagram is divided into two regions via the distillation boundary between azeotropes of EtAC/water and THF/water. In regions 1 and 2, all residue curves are directed from an unstable node to a stable node. Due to the existence of distillation boundary, it is impossible to separate the components by simple distillation. Figures 2 (b) and 2(c) show the RCMs with an effective entrainer. In Fig. 2(b), the intersection of the iso-volatility line and the EtAC-E edge is denoted as x_P. The position of x_P can be adopted to preliminarily evaluate the separation performance of the entrainer E. When a heaviest entrainer has a much stronger interaction with water (making EtAC the lightest component), the x_P point will be closer to the EtAC vertex, leading to a higher separation performance [45]. Additionally, the performance of the entrainer can be further verified via the intersection of the uni-volatility line and the EtAC-E edge. Water-EtAC-E indicates that water as a heavier component (in comparison with EtAC) can be distilled out from the top of the ED column when the total feed composition locates above the iso-volatility line. On the other hand, when the total feed composition is below the iso-volatility line, EtAC can be first distilled out. The analysis of the THF/water/E system in Fig. 2(c) is very similar to that of the EtAC/water/E system.

2.2 Conceptual design via RCMs

The ED process flowsheets can be designed via the analysis of the RCMs after the entrainer is determined. Normally, we can obtain two different process flowsheets with one following the direct separation sequence and the other following the indirect separation sequence.

2.3 Process optimization

The optimization of the ED process is carried out via the combination of the improved GA and Aspen Plus-based process simulation. Figure S1 (cf. ESM) demonstrates the scheme of the optimization process. Firstly, the discrete variables (e.g., feed locations), continuous variables (e.g., distillate rates and reflux ratios), and GA parameters (e.g., population size) are imported into an improved GA based software developed in our group. The first population is generated and sent to Aspen Plus to calculate the objective function and assess the constraints. In addition, the results are fed back to generate fitness function vectors, evaluate population and select the best individuals. The process optimization is terminated when the tolerance (difference between adjacent objective function values) satisfies the stop criteria. Otherwise, a new generation is created. The created generation is directly fed to Aspen Plus when there is no same individual in this generation; if not, mutation is imposed on one of them.

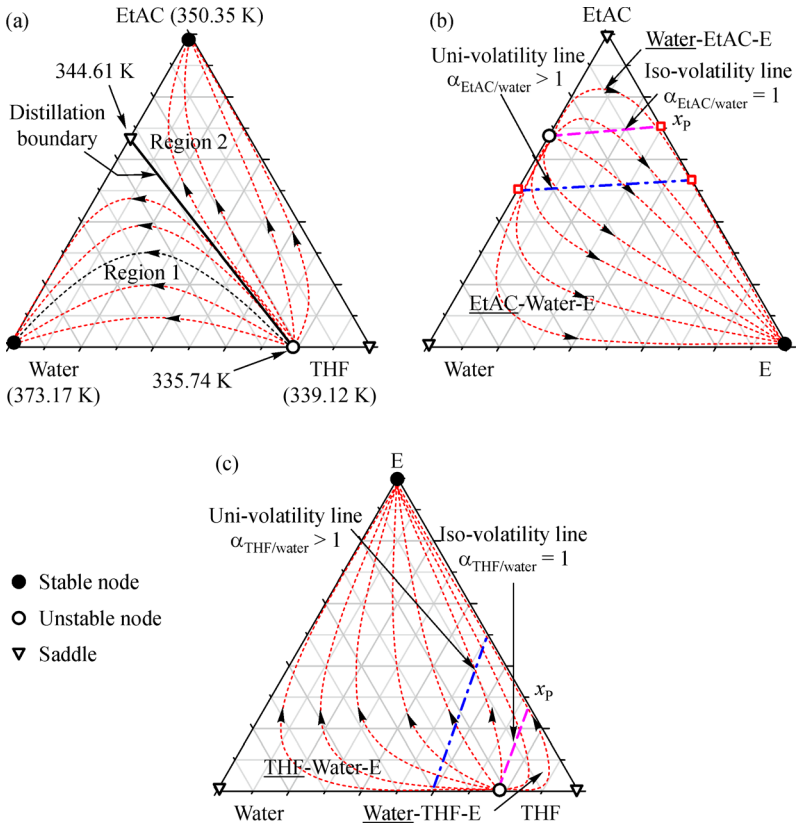

Fig. 2 RCMs of the (a) studied EtAC/THF/water system, (b) mixture of EtAC-water together with an entrainer E, and (c) THF-water with an entrainer E.

2.3.1 Objective function

In this work, the total annual cost (*TAC*) as illustrated in Eq. (6) is used to assess the economic performance of the proposed processes, which involves two parts: total capital cost (*TCC*) and annual operating cost (*AOC*) [46]. The *AOC* is made up of the steam and cooling water costs while the *TCC* includes the heat exchanger and distillation column costs. The payback period is assumed to be three years [47]. The detailed calculation of *TCC* and *AOC* could be found in the Supporting Information.

$$TAC = \frac{TCC}{\text{Payback period}} + AOC. \tag{6}$$

2.3.2 Constraints

In this work, three product purities and the entrainer purity in Eq. (7) are specified as constraints for the GA-based optimization.

$$x_{THF} \geqslant 99.50 \text{ mol-\%},$$

$$x_{EtAC} \geqslant 99.50 \text{ mol-\%},$$

$$x_{Water} \geqslant 99.50 \text{ mol-\%},$$

$$x_{Entrainer} \geqslant 99.50 \text{ mol-\%}. \tag{7}$$

2.3.3 Upper and lower bounds of decision variables

In the optimization process, upper and lower bounds of the discrete and continuous decision variables for the direct and indirect triple-column ED (TCED) processes are summarized in Table S2 (cf. ESM). There are eight integer decision variables including the total number of stages of the three columns (N_{T1}, N_{T2} and N_{T3}), feed locations of entrainers (N_{FE1} and N_{FE2}) and feed locations of the three columns (N_{F1}, N_{F2} and N_{F3}). Continuous decision variables include molar reflux ratios (RR_1, RR_2 and RR_3), flow rate of entrainer (F_E), split ratio of entrainer (SR), and distillate rates (D_1, D_2 and D_3).

2.4 Heat integration

The heat integration technique could be employed to reduce the process energy consumption when a sufficient temperature difference exists between the condenser and the reboiler [48].

3 Results and discussion

3.1 The entrainer screening

3.1.1 Results of CAMD

There are two binary azeotropes EtAC/water and THF/water in the ternary mixture EtAC/THF/water. In the UNIFAC-DMD model, EtAC is divided into three groups, CH_3, CH_2, and CH_3COO, and THF and water are single-group molecules. After the CAMD computation, dimethyl sulfoxide (DMSO), furfural and *N*,*N*-dimethylformamide (DMF) are identified as the most promising entrainers for all the different w_1 values (see Table S3, cf. ESM). According to the vapor-liquid equilibrium in Yang et al. [49], *N*-methyl-2-pyrrolidone (NMP) is an efficient solvent for separating the ternary mixture. Therefore, together with DMSO, DMF and furfural, NMP is considered as the fourth candidate entrainer to further verify the performance of the entrainers obtained from the CAMD.

3.1.2 Final determination of entrainer

The thermodynamic analyses such as iso- and uni-volatility lines are adopted to further determine the most powerful entrainer for the separation of the ternary azeotropic mixture EtAC/THF/water. The selection of thermodynamic model is important to accurately describe the vapor-liquid equilibrium of the system at different temperatures. Herein, the activity coefficient model UNIQUAC is employed and the corresponding binary interaction parameters are summarized in Table S4 (cf. ESM). Among the four entrainers, furfural is first excluded because it can form an extra azeotrope with water, leading to two separate distillation regions and thus making it incapable to separate THF/EtAC/water. For the other three entrainers, we performed a rigorous thermodynamic analysis, as discussed below.

Figure 3 displays the iso- and uni-volatility lines for azeotropes EtAC-water and THF-water using DMSO, NMP and DMF as the entrainers. These plots are generated via the separation module 'Flash 2' in Aspen Plus. As demonstrated, the entrainer DMSO shows a higher performance for the separation of EtAC/water and THF/water because its x_P point is closer to the components EtAC and THF, compared to the cases where NMP and DMF are used. Therefore, DMSO is finally selected as our entrainer for further process design and evaluation.

3.2 Conceptual design of the ED process

As seen in Figs. 3(a) and 3(c), the point of x_P locates on the edges of EtAC-DMSO and THF-DMSO indicating that EtAC and THF are more volatile than water when using

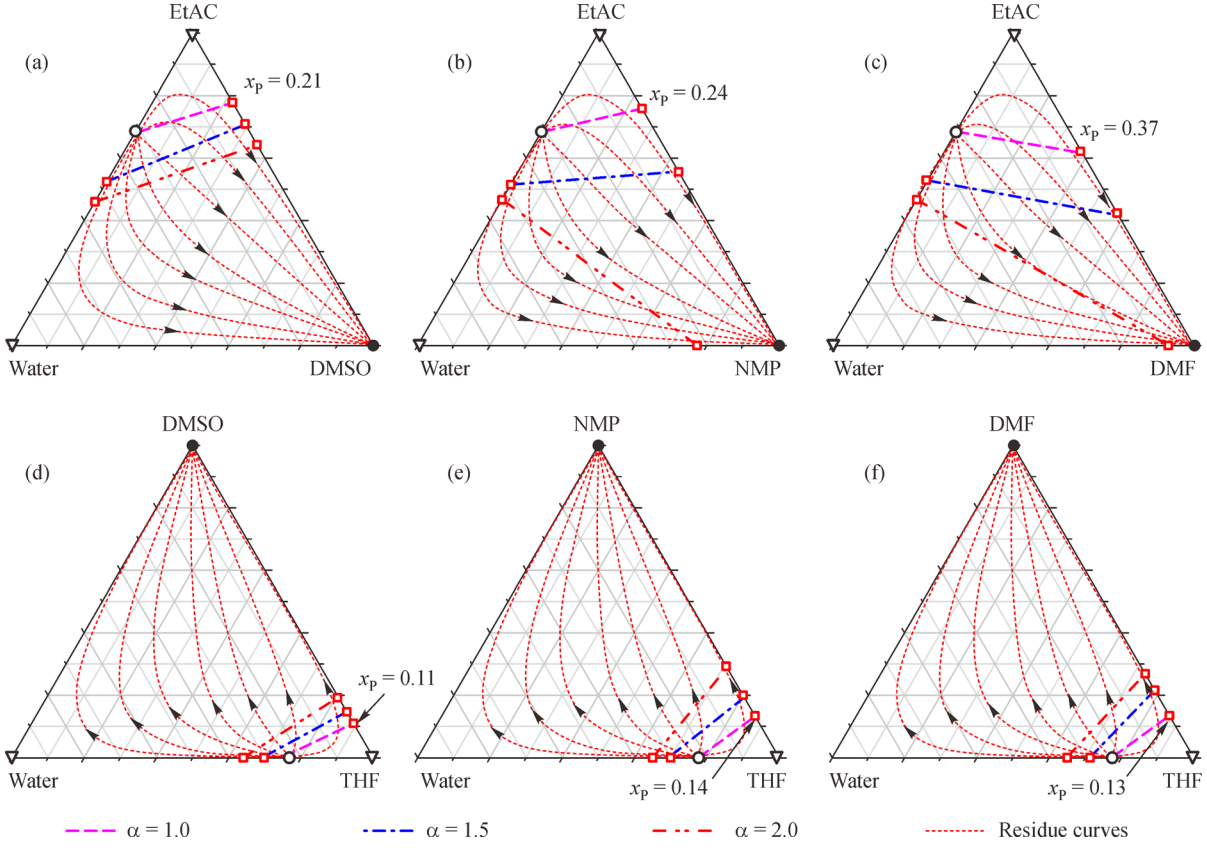

Fig. 3 The iso- and uni-volatility lines for (a–c) EtAC-water and (d–f) THF-water azeotropic mixtures by using different entrainers.

DMSO as the entrainer. Thereby, the component THF with the lowest boiling point can be firstly distilled out in an ED column when applying the direct separation sequence. Subsequently, EtAC can be obtained in another ED column and finally, water and DMSO can be separated in a conventional distillation column. In the indirect ED process, the mixture of THF and EtAC can be firstly obtained in an ED column and then separated in another distillation column. In summary, the separation of the ternary mixture THF/EtAC/water with two azeotropes can be achieved using DMSO as the entrainer via both the direct and indirect separation schemes.

3.2.1 Direct separation sequence

Figure 4 shows the direct TCED process for separating the ternary mixture THF/EtAC/water with two azeotropes. The process includes two ED columns (EDC1 and EDC2) and one entrainer recovery column (ERC). The entrainer DMSO is split into two substreams. One substream and the ternary mixture THF/EtAC/water are fed into EDC1 where THF and the mixture of EtAC/water/DMSO are distilled at the top and bottom, respectively. The mixture of EtAC/water/DMSO and the other entrainer substream are sent to EDC2 where EtAC and water/DMSO are obtained at the top and bottom, respectively. Finally, water and DMSO are separated in the ERC. SR denotes the ratio of the molar flow rate of the entrainer sent to EDC2 to the molar flow rate of the entire DMSO stream.

3.2.2 Indirect separation sequence

The indirect TCED process includes one EDC, one product distillation column (PDC) and one ERC (see Fig. 5). DMSO and the THF/EtAC/water mixture are fed into the EDC and then the mixtures of THF/EtAC and water/DMSO are obtained at the top and bottom of the EDC, respectively. The mixture of THF/EtAC enters the PDC and high purities of THF and EtAC are obtained at the top and bottom of PDC, respectively. The entrainer DMSO is finally separated from water in ERC and recycled back to EDC.

In the indirect process, it is necessary to separate the THF-EtAC mixture. Figure S2 (cf. ESM) plots the T-*xy* diagram for THF-EtAC under 1.0 and 0.5 bar. As illustrated in Fig. S2(a), the high purity of THF could not be obtained at 1.0 bar because the vapor and liquid lines are extremely close to each other (see the blue circle). The corresponding T-*xy* diagram of this binary system under 0.5 bar is shown in Fig. S2(b). As indicated, to use such a reduced pressure makes this binary separation possible [50]. For the EDC in both direct and indirect processes, we chose to operate them at 0.5 bar as well because this can increase the relative volatility of both EtAC-water and THF-water systems (see the uni-volatility lines at 1.0 and 0.5 bar in Fig. S3, cf. ESM). To use an even lower pressure will dramatically increase the cost for vacuuming thus is not considered here. For the ERC column in both direct and indirect processes, the task is to separate water and DMSO. We plot the *x*–*y* diagram for this binary system in Fig. S4 (cf. ESM). As demonstrated, this binary mixture is easy to separate regardless of the operating pressure. Herein, 0.5 bar is selected again because keeping the same pressure level as the previous columns can save pumping cost. Moreover, a reduced operating pressure in the ERC is also beneficial for decreasing the reboiler temperature, which helps save the cost for high-pressure steam. In

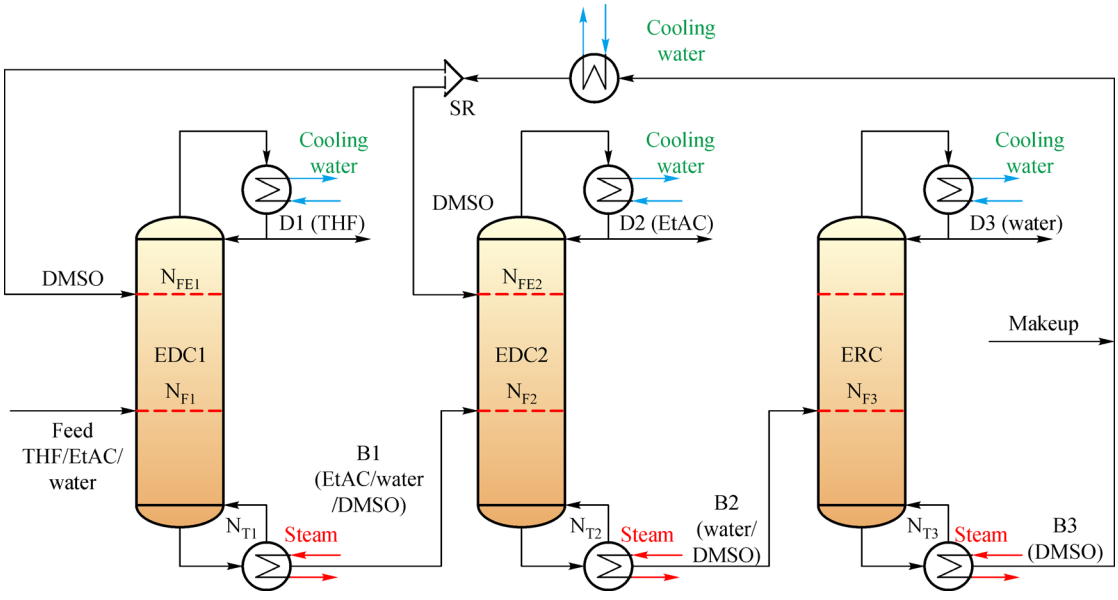

Fig. 4 The scheme of the direct TCED process for separating THF/EtAC/water.

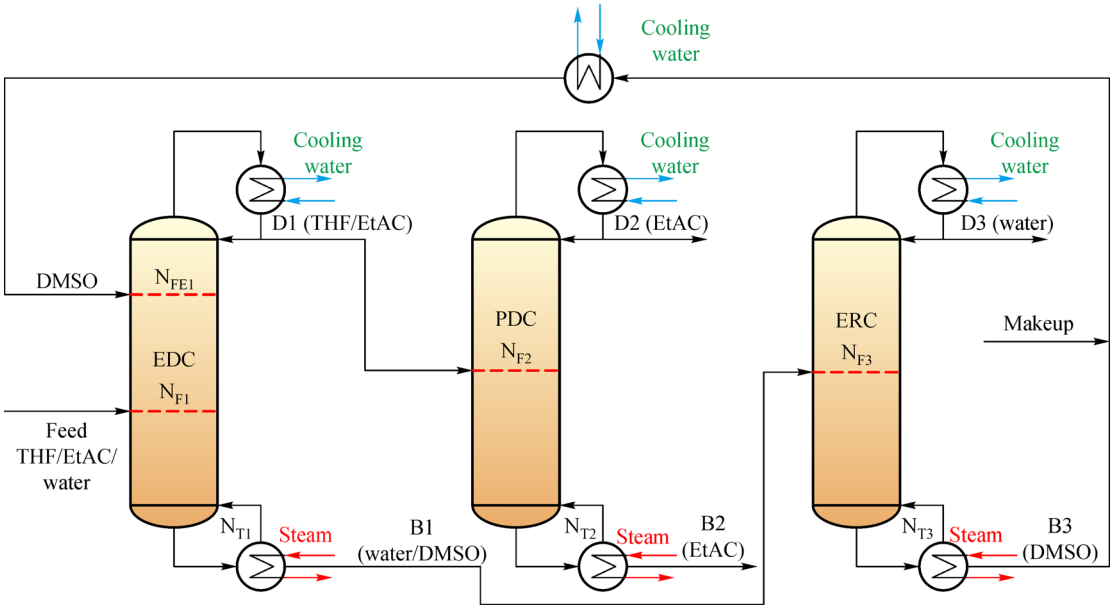

Fig. 5 The scheme of the indirect TCED process for separating THF/EtAC/water.

summary, all the distillation columns are operated at 0.5 bar.

3.3 Process optimization results

The optimization of the two proposed processes is implemented in the desktop computer with Intel® Core™ i7-7700 CPU@3.60 GHz and 8G RAM. Table S5 (cf. ESM) summarizes the setup parameters of the improved GA used in the optimization process as suggested by our previous work [41].

3.3.1 Direct TCED process

Figure 6 illustrates the dependence of the TAC of the direct TCED process on the number of generations. The optimization is stopped at 400 generations because the tolerance is lower than 10^{-5}. The whole process takes 1108 min. The optimal direct TCED process for separating the ternary azeotropic mixture THF/EtAC/water is demonstrated in Fig. 7 where all the stream information and column specifications are provided.

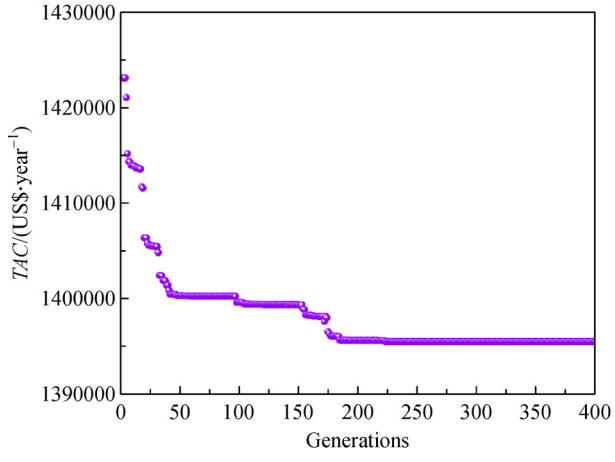

Fig. 6 The optimization result of the direct TCED process.

Figure S5 (cf. ESM) shows the liquid composition and temperature profiles of the optimal direct separation process. As demonstrated, THF, EtAC and water with high-purities are respectively distilled at the top of EDC1, EDC2 and ERC (Stage 1 of Figs. S5(a), S5(c) and S5(e)). The DMSO with 99.99 mol-% is obtained at the bottom of ERC. Moreover, temperature transitions can be observed near (or at) the feed locations, as shown in Figs. S5(b), S5(d) and S5(f).

3.3.2 Indirect TCED process

The reduction of TAC with number of generations for the indirect TCED process is given in Fig. 8. As shown, the optimization is terminated at 180 generations when the tolerance is lower than 10^{-5}. The whole calculation takes about 602 min.

Figure 9 illustrates the optimal indirect TCED process for separating the ternary azeotropic mixture THF/EtAC/water. The total number of stages of EDC, PDC and ERC are 16, 33 and 15, respectively. The entrainer DMSO and the ternary mixture are fed into the 5th and 12th trays of EDC while the feed locations of PDC and ERC are the 13th and 5th stages, respectively. To achieve the separation of THF/EtAC and water, 63.006 kmol·h^{-1} of DMSO and 0.1566 of reflux ratio are required in the EDC. High purities of THF and EtAC (i.e., 99.7 and 99.5 mol-%) are

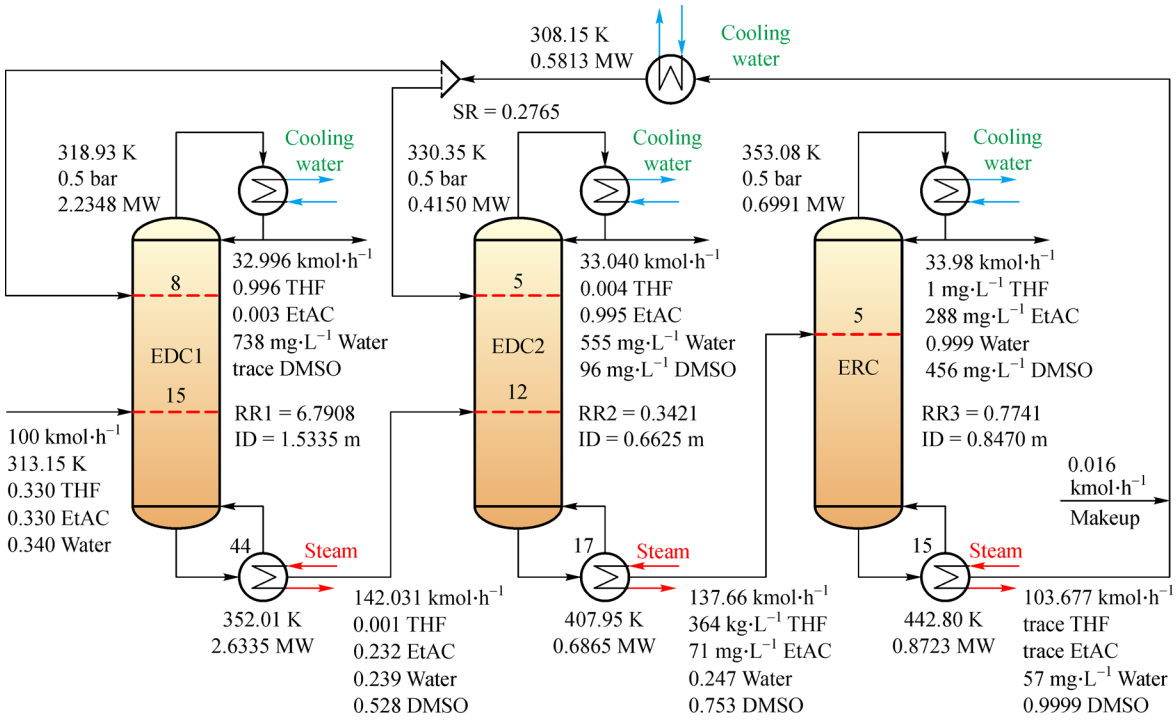

Fig. 7 The optimal direct TCED process for separating THF/EtAC/water using DMSO as the entrainer.

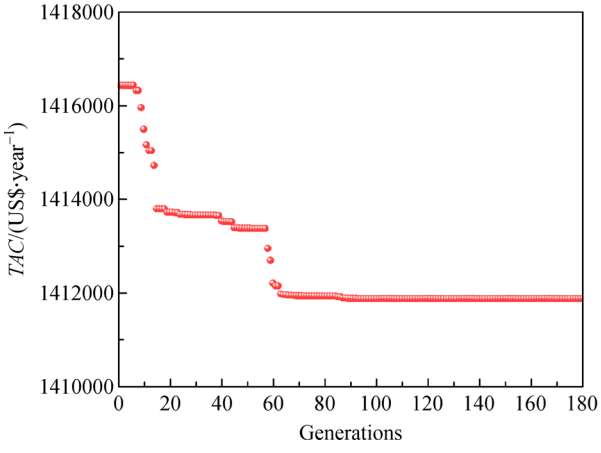

Fig. 8 The optimization results of the indirect TCED process.

obtained at the top and bottom of PDC. Water and DMSO are finally separated in the ERC column with 0.3833 of reflux ratio. The condenser duties of the three columns are 0.8879, 2.1898, and 0.5454 MW while the corresponding reboiler duties are 1.1935, 2.3763, and 0.6887 MW, respectively.

The liquid composition and temperature profiles of the indirect TCED process are displayed in Fig. S6 (cf. ESM). As indicated, THF/EtAC and water are separated at the extractive section (from 5th to 12th tray) while the concentrations of THF and EtAC get accumulated towards the top of the ED column. Notably, remixing occurs in the stripping section, resulting in more heat input. The composition and temperature profiles in PDC and ERC are easy to interpret because both of the columns separate binary mixtures.

3.4 Heat integration results

As illustrated in Fig. 7, the heat integration technology could not be employed for the direct TCED process because the difference between the temperature in the condenser (353.08 K) and the temperature in the reboiler (352.01 K) is too small. However, heat integration can be adopted to further reduce the energy consumption of the indirect TCED process because the temperature difference between the top of ERC and the bottom of PDC is higher than 14 K, as shown in Fig. 9.

Figure 10 depicts the optimal indirect TCED process where heat integration is applied. As shown, the reboiler duty of the PDC can be divided into two parts with 0.5454 MW supplied by the top vapor stream of the ERC and 1.8309 MW provided by an external steam. In other words, we can save 0.5454 MW heating and cooling duties by employing heat integration.

3.5 Comparison and discussions

The economic performance for the direct and indirect processes without and with heat integration is summarized in Table 2. The TAC of the three processes are 1397320.33, 1413626.41 and 1373366.41 US$·year^{-1}, respectively. As indicated, the proposed direct separation process with

99.6 mol-% THF purity shows a higher performance than the indirect one because it can avoid the repeat heating of components. Of note is that, a relatively higher THF purity (99.7 mol-%) and economic performance could be achieved via the indirect TCED process after heat integration is employed.

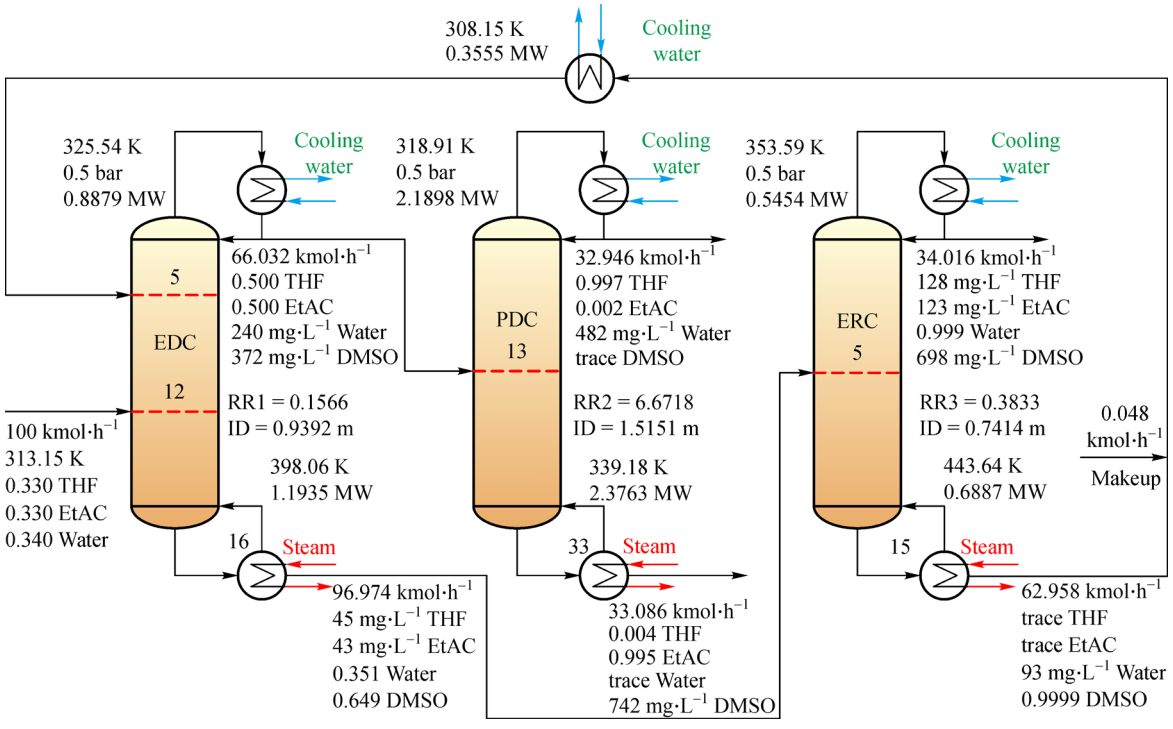

Fig. 9 The optimal indirect TCED process for separating THF/EtAC/water using DMSO as the entrainer.

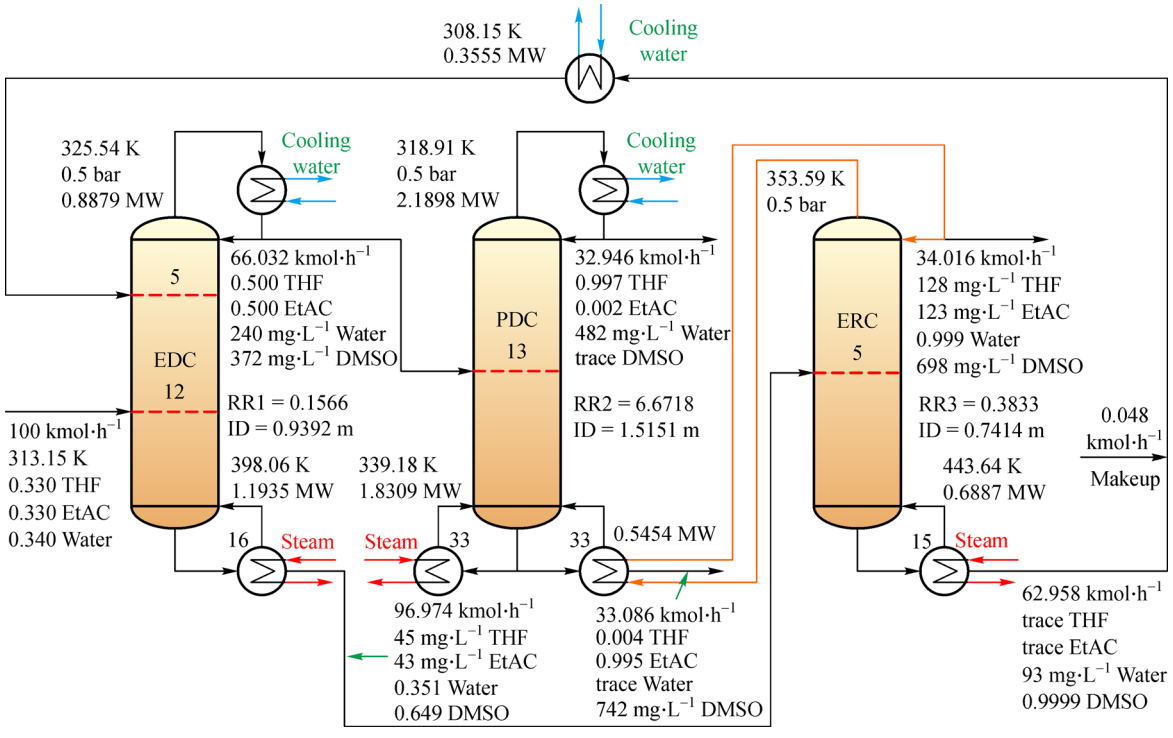

Fig. 10 The optimal indirect TCED process with heat integration for separating THF/EtAC/water using DMSO as the entrainer.

Table 2 Economic performance of the direct and indirect processes with and without heat integration

Item	Direct process	Indirect process without heat integration	Indirect process with heat integration
TCC/US$	1219334.38	1229563.80	1141299.66
AOC/(US$·year^{-1})	990875.54	1003771.81	992933.19
TAC/(US$·year^{-1})	1397320.33	1413626.41	1373366.41

4 Conclusions

In this contribution, an energy-efficient TCED process is developed for recovering THF and EtAC from industrial wastewater. A rigorous hierarchical design procedure involving entrainer design, thermodynamic analysis, process design and optimization, and heat integration is followed in the process development. First, candidate entrainers are screened via the CAMD method, and then the most efficient entrainer DMSO is determined via the comparison of the iso- and uni-volatility lines. Later, two alternatives of direct and indirect TCED processes are proposed. An improved GA is employed to optimize the proposed two processes. Heat integration is finally performed for the optimized processes. The TAC of the direct TCED process, indirect process without and with heat integration are 1397320.33, 1413626.41 and 1373366.41 US$·year^{-1}, respectively, which proves that the indirect separation process with heat integration is the best process alternative for separating THF/EtAC/water.

In order to reduce the remixing effects of the direct and indirect processes, intensified configurations such as dividing wall column and side-stream ED will be explored in the future work. In addition, innovative solvents such as ionic liquids will be considered in the entrainer design to find a potentially better ED process. Finally, life cycle environmental assessment can be included in the optimal process design.

Acknowledgements This work is financially supported by the National Key Research and Development Project (Grant No. 2019YFC0214403), the Joint Supervision Scheme with the mainland, Taiwan and Macao Universities (Grant No. SB2S to Yang A).

Electronic Supplementary Material Supplementary material is available in the online version of this article at http://dx.doi.org/10.1007/s11705-021-2044-z and is accessible for authorized users.

References

1. Santaella M A, Orjuela A, Narváez P C. Comparison of different reactive distillation schemes for ethyl acetate production using sustainability indicators. Chemical Engineering and Processing, 2015, 96: 1–13
2. Tran L S, Verdicchio M, Monge F, Martin R C, Bounaceeur R, Sirjean B, Glaude P A, Alzueta M U, Battin Leclerc F. An experimental and modeling study of the combustion of tetrahydrofuran. Combustion and Flame, 2015, 162(5): 1899–1918
3. He Z, Lin S, Gong C, Xi Y. Study on separating tetrahydrofuran from the mixture made up tetrahydrofuran, ethyl acetate and water. Journal of Shenyang Institute of Chemical Technology, 1996, 10(2): 143–147
4. Deorukhkar O A, Deogharkar B S, Mahajan Y S. Purification of tetrahydrofuran from its aqueous azeotrope by extractive distillation: pilot plant studies. Chemical Engineering and Processing, 2016, 105: 79–91
5. Yin Y, Yang Y, De Lourdes Mendoza M, Zhai S, Feng W, Wang Y, Gu M, Cai L, Zhang L. Progressive freezing and suspension crystallization methods for tetrahydrofuran recovery from Grignard reagent wastewater. Journal of Cleaner Production, 2017, 144: 180–186
6. Zhang X, He J, Cui C, Sun J. A systematic process synthesis method towards sustainable extractive distillation processes with preconcentration for separating the binary minimum azeotropes. Chemical Engineering Science, 2020, 227: 115932
7. Graczová E, Šulgan B, Barabas S, Steltenpohl P. Methyl acetatemethanol mixture separation by extractive distillation: economic aspects. Frontiers of Chemical Science and Engineering, 2018, 12(4): 670–682
8. Wang C, Zhang Z, Zhang X, Guang C, Gao J. Comparison of pressure-swing distillation with or without crossing curved-boundary for separating a multiazeotropic ternary mixture. Separation and Purification Technology, 2019, 220: 114–125
9. Liang S, Cao Y, Liu X, Li X, Zhao Y, Wang Y, Wang Y. Insight into pressure-swing distillation from azeotropic phenomenon to dynamic control. Chemical Engineering Research & Design, 2017, 117: 318–335
10. Han Z, Ren Y, Li H, Li X, Gao X. Simultaneous extractive and azeotropic distillation separation process for production of PODEn from formaldehyde and methylal. Industrial & Engineering Chemistry Research, 2019, 58(13): 5252–5260
11. Haaz E, Szilagyi B, Fozer D, Toth A J. Combining extractive heterogeneous-azeotropic distillation and hydrophilic pervaporation for enhanced separation of non-ideal ternary mixtures. Frontiers of Chemical Science and Engineering, 2020, 14(5): 913–927
12. Yang A, Shen W, Wei S, Dong L, Li J, Gerbaud V. Design and control of pressure-swing distillation for separating ternary systems with three binary minimum azeotropes. AIChE Journal. American Institute of Chemical Engineers, 2019, 65(4): 1281–1293
13. Li W, Zhong L, He Y, Meng J, Yao F, Guo Y, Xu C. Multiple steady-states analysis and unstable operating point stabilization in homogeneous azeotropic distillation with intermediate entrainer. Industrial & Engineering Chemistry Research, 2015, 54(31): 7668–7686
14. Gerbaud V, Rodriguez Donis I, Hegely L, Lang P, Denes F, You X. Review of extractive distillation. Process design, operation,

optimization and control. Chemical Engineering Research & Design, 2019, 141: 229–271
15. Li H, Wu Y, Li X, Gao X. State-of-the-art of advanced distillation technologies in China. Chemical Engineering & Technology, 2016, 39(5): 815–833
16. Yang A, Sun S, Shi T, Xu D, Ren J, Shen W. Energy-efficient extractive pressure-swing distillation for separating binary minimum azeotropic mixture dimethyl carbonate and ethanol. Separation and Purification Technology, 2019, 229: 115817
17. Shi T, Yang A, Jin S, Shen W, Wei S, Ren J. Comparative optimal design and control of two alternative approaches for separating heterogeneous mixtures isopropyl alcohol-isopropyl acetate-water with four azeotropes. Separation and Purification Technology, 2019, 225: 1–17
18. Pan Q, Shang X, Li J, Ma S, Li L, Sun L. Energy-efficient separation process and control scheme for extractive distillation of ethanol-water using deep eutectic solvent. Separation and Purification Technology, 2019, 219: 113–126
19. Shi X, Zhu X, Zhao X, Zhang Z. Performance evaluation of different extractive distillation processes for separating ethanol/tert-butanol/water mixture. Process Safety and Environmental Protection, 2020, 137: 246–260
20. Yang A, Zou H, Chien I L, Wang D, Wei S, Ren J, Shen W. Optimal design and effective control of triple-column extractive distillation for separating ethyl acetate/ethanol/water with multiazeotrope. Industrial & Engineering Chemistry Research, 2019, 58(17): 7265–7283
21. Cignitti S, Rodriguez-Donis I, Abildskov J, You X, Shcherbakova N, Gerbaud V. CAMD for entrainer screening of extractive distillation process based on new thermodynamic criteria. Chemical Engineering Research & Design, 2019, 147: 721–733
22. Woo H C, Kim Y H. Solvent selection for extractive distillation using molecular simulation. AIChE Journal. American Institute of Chemical Engineers, 2019, 65(9): e16665
23. Cui Y, Zhang Z, Shi X, Guang C, Gao J. Triple-column side-stream extractive distillation optimization via simulated annealing for the benzene/isopropanol/water separation. Separation and Purification Technology, 2020, 236: 116303
24. Zhu Z, Li G, Dai Y, Cui P, Xu D, Wang Y. Determination of a suitable index for a solvent via two-column extractive distillation using a heuristic method. Frontiers of Chemical Science and Engineering, 2020, 14(5): 824–833
25. Shen W, Dong L, Wei S, Li J, Benyounes H, You X, Gerbaud V. Systematic design of an extractive distillation for maximum-boiling azeotropes with heavy entrainers. AIChE Journal. American Institute of Chemical Engineers, 2015, 61(11): 3898–3910
26. Blahušiak M, Kiss A A, Babic K, Kersten S R A, Bargeman G, Schuur B. Insights into the selection and design of fluid separation processes. Separation and Purification Technology, 2018, 194: 301–318
27. Gani R, Brignole E. Molecular design of solvents for liquid extraction based on UNIFAC. Fluid Phase Equilibria, 1983, 13: 331–340
28. Gertig C, Kröger L, Fleitmann L, Scheffczyk J, Bardow A, Leonhard K. Rx-COSMO-CAMD: computer-aided molecular design of reaction solvents based on predictive kinetics from quantum chemistry. Industrial & Engineering Chemistry Research, 2019, 58(51): 22835–22846
29. Liu Q, Zhang L, Liu L, Du J, Meng Q, Gani R. Computer-aided reaction solvent design based on transition state theory and COSMO-SAC. Chemical Engineering Science, 2019, 202: 300–317
30. Zhou T, Wang J, McBride K, Sundmacher K. Optimal design of solvents for extractive reaction processes. AIChE Journal. American Institute of Chemical Engineers, 2016, 62(9): 3238–3249
31. Zhang L, Pang J, Zhuang Y, Liu L, Du J, Yuan Z. Integrated solvent-process design methodology based on COSMO-SAC and quantum mechanics for TMQ (2,2,4-trimethyl-1,2-H-dihydroquinoline) production. Chemical Engineering Science, 2020, 226: 115894
32. Song Z, Zhang C, Qi Z, Zhou T, Sundmacher K. Computer-aided design of ionic liquids as solvents for extractive desulfurization. AIChE Journal. American Institute of Chemical Engineers, 2018, 64 (3): 1013–1025
33. Chao H, Song Z, Cheng H, Chen L, Qi Z. Computer-aided design and process evaluation of ionic liquids for *n*-hexane-methylcyclopentane extractive distillation. Separation and Purification Technology, 2018, 196: 157–165
34. Zhou T, Song Z, Zhang X, Gani R, Sundmacher K. Optimal solvent design for extractive distillation processes: a multiobjective optimization-based hierarchical framework. Industrial & Engineering Chemistry Research, 2019, 58(15): 5777–5786
35. Silva R O, Torres C M, Bonfim Rocha L, Lima O C M, Coutu A, Jiménez L, Jorge L M M. Multi-objective optimization of an industrial ethanol distillation system for vinasse reduction—a case study. Journal of Cleaner Production, 2018, 183: 956–963
36. Waltermann T, Grueters T, Muenchrath D, Skiborowski M. Efficient optimization-based design of energy-integrated azeotropic distillation processes. Computers & Chemical Engineering, 2020, 133: 106676
37. Krone D, Esche E, Asprion N, Skiborowski M, Repke J U. Conceptual design based on superstructure optimization in GAMS with accurate thermodynamic models. Computer-Aided Chemical Engineering, 2020, 48: 15–20
38. Li X, Cui C, Li H, Gao X. Process synthesis and simulation-based optimization of ethylbenzene/styrene separation using double-effect heat integration and self-heat recuperation technology: a techno-economic analysis. Separation and Purification Technology, 2019, 228: 115760
39. Su Y, Jin S, Zhang X, Shen W, Eden M R, Ren J. Stakeholder-oriented multi-objective process optimization based on an improved genetic algorithm. Computers & Chemical Engineering, 2020, 132: 106618
40. Kruber K F, Grueters T, Skiborowski M. Efficient design of intensified extractive distillation processes based on a hybrid optimization approach. Computer-Aided Chemical Engineering, 2019, 46: 859–864
41. Yang A, Su Y, Chien I L, Jin S, Yan C, Wei S, Shen W. Investigation of an energy-saving double-thermally coupled extractive distillation for separating ternary system benzene/toluene/cyclohexane. Energy, 2019, 186: 115756
42. You X, Gu J, Gerbaud V, Peng C, Liu H. Optimization of pre-concentration, entrainer recycle and pressure selection for the

extractive distillation of acetonitrile-water with ethylene glycol. Chemical Engineering Science, 2018, 177: 354–368

43. Momoh S O. Assessing the accuracy of selectivity as a basis for solvent screening in extractive distillation processes. Separation Science and Technology, 1991, 26(5): 729–742
44. Marrero J, Gani R. Group-contribution based estimation of pure component properties. Fluid Phase Equilibria, 2001, 183: 183–208
45. Rodriguez Donis I, Gerbaud V, Joulia X. Thermodynamic insights on the feasibility of homogeneous batch extractive distillation, 1. azeotropic mixtures with a heavy entrainer. Industrial & Engineering Chemistry Research, 2009, 48(7): 3544–3559
46. Douglas J M. Conceptual Design of Chemical Processes. 1st ed. New York: McGraw-Hill, 1988, 461–462
47. Luyben W L. Distillation Design and Control Using Aspen Simulation. 1st ed. New Jersey: John Wiley & Sons, 2013, 87–89
48. Zhang Q, Liu M, Li C, Zeng A. Heat-integrated pressure-swing distillation process for separation of the maximum-boiling azeotrope diethylamine and methanol. Journal of the Taiwan Institute of Chemical Engineers, 2018, 93: 644–659
49. Yang J, Pan X, Yu M, Cui P, Ma Y, Wang Y, Gao J. Vaporliquid equilibrium for binary and ternary systems of tetrahydrofuran, ethyl acetate and *N*-methyl pyrrolidone at pressure 101.3 kPa. Journal of Molecular Liquids, 2018, 268: 19–25
50. Xia M, Shi H, Niu C, Ma Z, Lu H, Xiao Y, Hou B, Jia L, Li D. The importance of pressure-sensitive pinch/azeotrope feature on economic distillation design. Separation and Purification Technology, 2020, 250: 116753